Optimization of Cutting Parameters for Finish end Milling CFRP Under Vortex-Cooled Compressed Air

Rodrigo F. Klein[a], Nícholas Hoffmann[a], André J. Souza[a]* , Franciele J. Rebelo[a],

Heraldo J. Amorim[a]

[a]Universidade Federal do Rio Grande do Sul, Departamento de Engenharia Mecânica, Laboratório de Automação em Usinagem, Porto Alegre, RS, Brasil.

Carbon fiber reinforced plastics (CFRP) offer several advantages in the aeronautical and automotive industry due to their combination of lightweight, high strength, and corrosion resistance. CFRP parts are usually produced in near-net-shape; however, additional machining processes are often required for achieving desired dimensional accuracy and surface finish. Thus, this work evaluates the influence of the cutting parameters in CFRP end milling to generate a better surface finish. The experiment was designed using a three-factor, three-level Box-Behnken considering feed rate (f), axial depth of cut (a_p), and cooling conditions (cc) as controllable factors, and roughness parameters (R_a, R_q, R_z, R_t) as response variables (the occurrence of defects was evaluated qualitatively). Results indicated a strong influence of the quadratic effect of axial depth of cut and its interactions with feed rate and cooling condition on the roughness values and a milder but significant influence of the feed rate and cooling conditions. Multivariate analysis returned the optimum level of input parameters (f = 0.21 mm/rev and a_p = 0.8 mm with cooled compressed air), resulting in R_a = 1.58 µm, R_q = 1.98 µm, R_z = 9.39 µm, R_t = 13.63 µm. Also, no defects were observed after machining under the optimum conditions.

Keywords: *Carbon fiber reinforced plastic, end milling, surface roughness, vortex-cooled compressed air.*

1. Introduction

Carbon fiber reinforced polymer (CFRP) are composite materials in which fibers with high tensile and compressive strength, stiffness, and excellent fatigue characteristics[1] are combined with a matrix that holds the fibers in their proper position and provides corrosion and abrasion protection while allowing load transfer between fibers and providing interlaminar shear strength[2]. Thus, while the fiber reinforcements and the matrix keep their physical and chemical identities, their combination results in a set of properties that cannot be achieved separately: the main characteristics of CFRP are high strength per weight ratio, high damping capacity, good dimensional stability, excellent damage resistance, and good corrosion and fatigue resistance. The good properties of CFRP have made this material widely used in aerospace, automotive, and military industries. Recent applications of these composite materials include wind turbines, construction, bicycles, sports, and home appliances[3,4].

Composite matrices may consist of polymeric, metallic, or ceramic materials. Fiber-reinforced plastics such as CFRP use thermoplastics or thermosetting polymeric resin matrices, with the latter being more used due to its better mechanical properties and lower cost[5]. Also, CFRP can be classified according to its fiber direction, which can be unidirectional, bidirectional, or multidirectional (unidirectional layers stacked in different directions)[6]. Components based on CFRP are usually produced in near net shape by the molding methods (by compression or in an autoclave) or filament winding[7]. Currently, much of the manufacture of CFRP parts uses pre-impregnated (prepreg) fabrics or tapes, which are composite materials whose fiber mesh is impregnated with uncured resin by the material supplier, thus only requiring molding and final curing[1]. However, complementary machining processes (milling, drilling, or turning) are frequently used to achieve the desired dimensions and tolerances[8-10].

Due to their heterogeneous structure, CFRP machining differs significantly from the conventional machining of metals, with different material damage mechanisms[11,12]. Despite its growing use, CFRP milling remains a challenging process, potentially causing several defects on the part that may lead to waste: the lack of homogeneity and anisotropy of CFRP can lead to fiber pullout[13] and bending during machining[14]. The abrasive nature of the fibers may also lead to premature tool wear, inducing damages such as delamination, debonding, fiber pullout, and cracking of the matrix[14-16]. The chip formation process in CFRP machining consists of a series of brittle fractures and is strongly dependent on the orientation of the fibers in the material[7]. The cutting action occurs with the detachment and folding of the fiber until it ruptures, forming a chip. The process repeats itself, generating a surface texture composed of exposed fibers and resin ridges, separating fibers and resin. Then, fiber orientation significantly affects chip formation and the resulting surface roughness[4,17]. Several studies reported that feed rate[16,18-22] and fiber (ply) orientation angle[4,17,18,23-25] are the most significant

factors in the surface finish generated by milling of FRP. The roughness values grew with the increase in feed rate[22] and when the ply orientation was changed from 45° to 135°[25].

Several studies investigated the influence of the machining parameters on the surface roughness resulting from the machining of fiber-reinforced plastics (FRP). According to Sreenivasulu[20], the increase in the depth of cut (a_p) harmed the surface quality in milling glass-fiber-reinforced plastic (GFRP). Zhou et al.[26] observed that a_p is the most influential parameter on the surface roughness of milled CFRP, and its increase deteriorates the surface quality. The multiple layers of epoxy resin are hard to remove and can adhere to the machined surface due to the combined effect of force and heat generated by the cutting tool action. Gao et al.[25] also observed that the increase of a_p in the CFRP milling results in the growth of the cutting forces and negatively affects the surface roughness. The authors noted a large dispersion of the mean roughness (R_a) values at higher a_p and associated this phenomenon with the characteristics of the material. Çolak and Sunar[27] and Yashiro et al.[28] reported that feed rate (f) is the cutting parameter that has the most significant statistical influence on the CFRP surface roughness and delamination generated by milling, as smaller values of feed rate reduce the roughness values by decreasing surface damages caused by the process. Similar results were reported by Azmi et al.[21] for end milling of GFRP (glass fiber reinforced polymer). However, as pointed out by El-Hofy et al.[29], high cutting speeds (v_c) and high feed per tooth (f_z) reduce machining time. At this rate, the increase in v_c leads to higher temperatures, while high f_z acts oppositely due to the lower contact between the tool and the part. Thus, the combination of high f_z and v_c may be allowed an increase in production while reducing the occurrence of temperature-related damages. Nor Khairusshima et al.[30] also concluded that the best surface quality in CFRP milling is reached with high v_c and f levels. Similar results were presented by Voss et al.[18], who also observed that larger clearance and rake tool angles improve the surface quality and reduce tool wear. Devitte et al.[31] evaluated the influence of the cutting parameters and tool geometry in the delamination in Al-GFRP-Al hybrid stack drilling. The best results were achieved using lower v_c, f, and a drill with a lower point angle, lower chisel edge, and higher rake angle.

The abrasive nature of the carbon fibers leads to high tool wear rates in machining processes: chips and fibers act as abrasive particles during the cutting. Thus, the continuous friction with the cutting tool causes abrasive wear[18]. This failure harms the surface quality of the machined part and reduces productivity due to frequent tool changes and additional machining requirements, thus increasing production costs. Due to these hindrances, different tool materials are used in the machining of CFRP, such as uncoated carbide[22] and coated polycrystalline diamond[25,32]. Hence, the main targets of several research papers are reducing tool wear and improving surface finish in CFRP machining[3,33].

Fracturing composites do not require as much energy as shearing metals; thus, the cutting forces and temperatures observed in the machining of these materials are much lower[29]. These low temperatures eliminate diffusion wear during the machining of CFRP[34]. However, carbon fiber reinforced polymers present low thermal conductivity, and thermal defects generated by friction between the cutting tool and the laminated composite may affect the material properties, especially the polymer matrix[35]. The low thermal conductivity can also lead to thermal defects in the machined part, with the quality of the machined surface decreasing with the increase of the temperature in the cutting zone. High temperatures may also cause a decrease in the matrix stiffness, which potentially induces damages such as delamination, fiber pullout, transversal cracks, porosity, and pits[36,37]. Extreme machining conditions may lead to temperatures above the glass transition temperature of the polymer matrix, leading the softened polymer and carbon fibers to form an irregular surface[38]. El-Hofy et al.[29] investigated the temperatures in the CFRP slot milling. The authors reported temperatures ranging from 193°C to 207°C for new tools, with increased flank wear until VB = 0,1 mm. Devitte et al.[39] investigated the temperatures developed in dry CFRP drilling. The authors observed a maximum temperature of 49.9 °C, below the reported grass transition point. Pecat et al.[24] investigated the surface finish based on the analysis of cross-section micrographs of the milled surface of CFRP for parts machined at four different temperatures (-40 °C, 20 °C, 80 °C, and 120 °C). The authors observed sub-surface damage in parts machined at the lower tested temperatures and attributed this effect to the brittleness of the matrix material in these conditions. A severe sub-surface alteration was observed when the working temperature was 120 ºC. The authors concluded that the ideal temperature for CFRP milling is 80 ºC (below the glass-transition temperature "Tg" of epoxy resin); also, the smaller cutting forces were observed in this condition. Wang et al.[32] concluded that the matrix resin support for the fibers is unsuitable when the cutting temperature exceeds the glass transition temperature, which results in a low surface quality in the machining of composite materials. Consequently, the temperature during machining significantly influences the surface quality. Considering the effects of high temperatures in the machined part, it is safe to conclude that heat generation is a factor that hampers high productivity in CFRP machining.

Due to the harmful influence of high temperatures in CFRP, heat removal is desirable for machining defect-free parts with good surface quality and high productivity. However, conventional cutting fluids induce moisture absorption, affecting the properties and dimensions of the material, including separation between fiber and matrix and the generation of small valleys and cracks[29,40]. Different techniques are studied to replace conventional flood cooling in machining processes, including dry machining, compressed-air cooling, and minimal quantity of lubricant (MQL). Techniques involving compressed air are interesting when sustainability and economy are considered since they are based on a readily available medium.

Rodriguez et al.[41] compared the influence of different cooling methods in CFRP grinding. The authors performed tests with conventional (flood) lubrication, MQL, dry machining, and a technique that consisted of a high-pressure stream of a small quantity of lubricant, referred to in the study as optimized cooling. The study did not consider the moisture absorption of the stream-based methods, and the

best surface finishes were achieved with flood and optimized cooling. MQL presented the highest roughness values for all conditions, followed by dry machining. The authors link the result to inadequate cooling that led to the clogging of the grinding wheel surface. According to Xu et al.[42], the low efficiency of MQL is related to the quick absorption of the MQL droplets and the deficient lubrication due to this absorption since no lubricating film is formed. Also, due to the low temperatures compared with the metal machining, the heat removal because of the droplet's evaporation is not achieved in CFRP machining.

The use of vortex-cooled compressed air (VCCA) has been studied as an alternative for reducing the temperature in the cutting region[43]. This technique consists of the airstream application, whose temperature is reduced directly to the cutting area by a vortex tube. Hoffmann et al.[44] reported a considerable reduction of delamination in air-cooled CFRP drilling compared with dry cutting. Nor Khairusshima and Sharifah[45] studied the influence of this cooling method in CFRP milling, reporting longer tool lives with chilled air-assisted machining for all tested conditions. Lower tool lives were observed for the machining with high cutting speed (v_c) and high feed per tooth (f_z). Nor Khairusshima et al.[19] and Yalçin et al.[46] concluded that the roughness values generated by air-cooled assisted milling are lower than those achieved by dry machining. According to the authors, the refrigeration effect was more effective at high cutting speeds. There is better heat transfer by forced convection; furthermore, the cooled compressed air significantly affected the cut, especially with higher values of feed per tooth. However, Klein et al.[47] verified that high a_p combined with low f_z and low a_p with high f_z in dry milling of CFRP resulted in lower average roughness values than the machining with compressed air and VCCA. Despite the authors concluding that the strong influence of a_p on the quality of CFRP machined surface is related to the carbon fiber fracture and the resin exposure, the analysis was limited to the evaluation of the surface roughness R_a since no other method was used for the assessment of the surface quality as scanning electron microscopy (SEM). Thus, it is safe to conclude that the use of cooled compressed air increases the stiffness of the CFRP matrix, reducing the fiber pull out, delamination, and surface roughness[38,45].

The strength and fatigue resistance of machined components, especially in structural applications, is critically dependent on the quality of the surfaces produced by machining[48]. The surface irregularities, mainly valleys or grooves, are stress concentrators that facilitate the plastic deformation of the material and the formation of cracks. Therefore, smooth surfaces have a lower risk of initiating cracks[5], improving the fatigue resistance of the part[49]. The surface roughness also influences tribological characteristics by determining the actual area of contact between surfaces, influencing friction, wear and lubrication. Furthermore, the quality of surfaces is essential in applications that require optical, electrical, and thermal performance or in whose paint application and good appearance are necessary[5]. The quality of a machined surface is often characterized by surface morphology (or texture) and surface integrity. While texture considers the geometric characteristics of the generated surface, surface

integrity describes physical and chemical changes to the surface after machining, including fiber pullout, delamination, matrix removal, or decomposition[48].

Considering the obstacles involved in the end milling of CFRP, this work intends to statistically analyze the influence of axial depth of cut, feed rate, and cooling condition in the surface finish, thus contributing to a better understanding of this machining process. Using a response surface methodology (RSM) to evaluate the results allows a better understanding of the machining process and the optimization of cutting parameters.

2. Materials and Methods

2.1. Materials and equipment

The CFRP specimen used in this study is a carbon fiber-reinforced polymer matrix composite plate composed of 38 layers of 0.29 ± 0.04 mm thick pre-impregnated carbon epoxy bidirectional sheets, with fibers oriented at 0°/90° and glass-transition temperature of 130 °C. The final thickness of the plate is 8.7 ± 0.3 mm, with a variation due to the manufacturing process. This variation caused changes in the axial depth of cut (a_p). Thus, the a_{p-T} (intended theoric value) and a_{p-R} (measured real value) were defined for the end milling process. The experiments were performed with a ROMI Discovery 308 CNC machining center using a Kennametal F4AJ1000AWL30 K600 4-flute uncoated solid carbide end mill with a diameter of 10 mm and a helix angle of 30°. The tool has a radial rake angle of 30° and an axial rake angle of 0°.

Three cooling conditions (cc) were tested: dry cutting (DRY), regular compressed air (AIR) at 17 °C, and vortex-cooled compressed air (VCCA) at 6 °C, produced with a Turbo Air Eurotools FTA-12-MC. The use of vortex-cooled air was considered due to the non-linear influence of temperature in the machining of CFRP: while low temperatures cause the embrittlement of the matrix, leading to sub-surface defects, high temperatures soften the matrix, leading to damages like fiber pullout, as reported by Pecat et al.[24] The compressed air line pressure was 300 kPa for both AIR and VCCA, and both techniques were applied with a 6 mm cylindrical nozzle positioned at a distance of 30 mm from the cutting region. Figure 1 presents the experimental setup. It is worth mentioning that the fine particles generated in the machining of CFRP can be suspended in the air, resulting in potential health hazards for the operator[50], mainly when compressed air cooling is used. Consequently, it is strongly recommended to enclose the working area of the machine tool, preferably using an exhaustion system. Also, the operator must use a protective mask to further the other necessary individual protection equipment.

The end milling experiment performed 15 passes of 35 mm in the workpiece, as depicted in Figure 2. In addition, six validation passes were performed after optimization, resulting in 21 runs. The tested conditions were defined through Box-Behnken Design.

The surface roughness parameters R_a (average roughness), R_q (root-mean-square roughness), R_z (average peak-to-valley height), and R_t (total height of the roughness profile) generated by end milling CFRP were measured with a
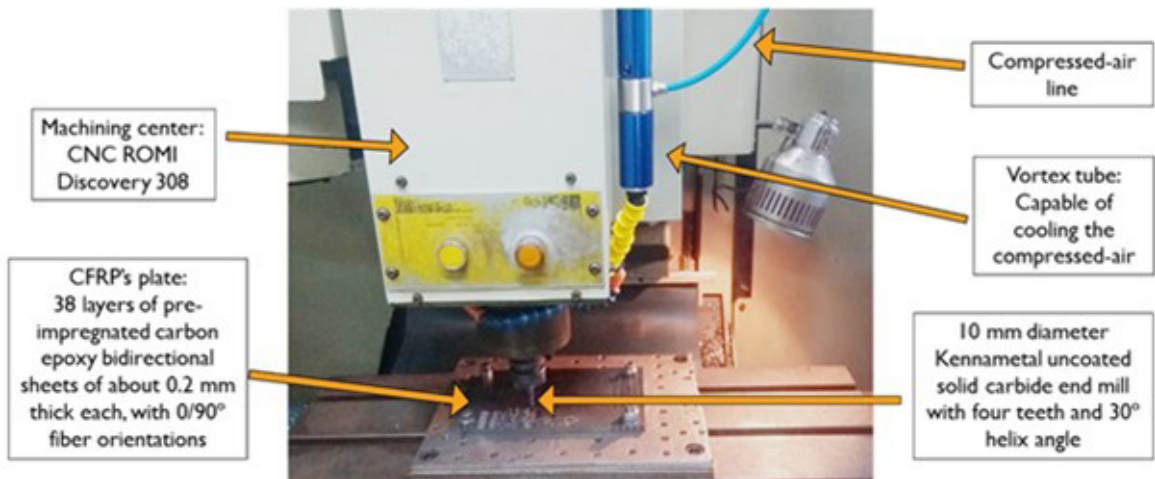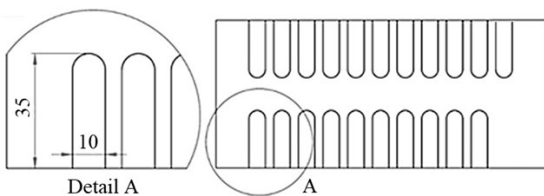
Figure 1. Experimental setup.

Figure 2. Details of the workpiece used in the experiment.

Mitutoyo Surftest SJ-201P portable stylus profilometer with a diamond stylus with 5 μm tip radius and resolution of 0.01 μm. These measurements considered a sampling length of $l_e = 2.5$ mm and an evaluation length of $l_m = 5 \cdot l_e = 12.5$ mm. According to DIN EN ISO 4288, these standard sampling and evaluation lengths for R_a and R_z from non-periodic roughness profiles are defined by ranges $2 < R_a \leq 10$ μm and $10 < R_z \leq 50$ μm. Each machined sample was measured in at least three points; in some cases, the number of points was increased for higher reliability due to the high dispersion of results. Finally, the arithmetic means of the measured results were calculated. The machined surfaces were also analyzed through scanning electron microscopy (SEM) using a Zeiss Evo Ma10 microscope. Each sample of the machined surface was cut, cleaned, and dried before image capture. The Bal-tec SCD 050 metallizer was used to create a gold film on the surfaces, thus improving the image quality.

Differences in the roughness values after end milling were reported by Gara and Tsoumarev[51], who observed better surface roughness in the up milling portion of the cut than in the portion where down milling occurred. Another possible explanation for the dispersion of the roughness values is the fiber orientation. Since it varies with the tool rotation, it affects different cutting regions differently, which affects the surface finish. According to Chatelain et al.[52], the fiber (ply) orientation critically affects the surface roughness of the laminate, and the worst case is found at 135°. It could be explained by a fiber bending that occurs during machining, which would be different for each ply orientation.

2.2. Design of experiments (DOE)

Box-Behnken Design (BBD) is a statistical optimization method that aims to simultaneously obtain the best levels in a set of factors that influence a specific response variable. This DOE combines factorial analysis with incomplete block designs and proposes three levels for each controllable factor to develop a response surface[53]. Several studies of machining composite materials use BBD[54-56] as it has the advantage of reducing the number of runs that need to be executed, generating lower consumption of materials, and reducing lab work.

A three-factor BBD was carried out to clarify the influence of the machining parameters on the surface quality in the end milling of CFRP. Three factors (f, a_p, and cooling condition) were tested in three levels according to Table 1. The cutting speed was kept constant throughout the tests. The chosen cutting speed ($v_c = 120$ m/min) considered the maximum allowed rotation of the machining center (4000 rpm) and the tool diameter (10 mm). In a complete 3^3 factorial design, it would be necessary to test 27 different conditions; when considering three replications, it would result in 81 runs. The use of BBD allowed reducing the number of runs to 15.

A reduced variance analysis (ANOVA) model was carried out using the Minitab® 19 software to quantify the linear and quadratic effects of each factor and their interactions on the response variables (R_a, R_q, R_z, R_t). A 95% confidence interval was considered (p-value < 0.05). The factor with a higher p-value was eliminated, and a new analysis was run. The procedure was repeated until all p-values were below 5% (to ensure a 95% confidence) or until the coefficient of determination $R^2 > 70\%$ (assuming a maximum error of 30%) was reached. After statistical processing, Response Surface Methodology (RSM) was used for modeling the behavior of the roughness parameters based on the control variables, followed by the optimization of controllable input factors using the Minitab® 19. Finally, validation tests were executed with the optimal levels.

Table 1. Factors and levels used in BBD.

Controllable Factors	Notation	Unit	Levels		
			Low (-1)	Medium (0)	High (+1)
Axial depth of cut (theoric)	$a_{p\text{-}T}$	mm	0.6	1.0	1.4
Feed rate	f	mm/rev.	0.07	0.14	0.21
Cooling conditions	cc	-	DRY	AIR	VCCA
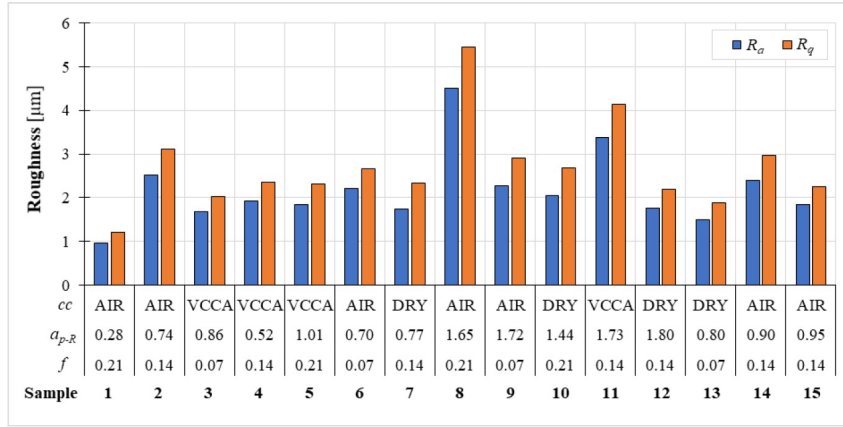
(a)
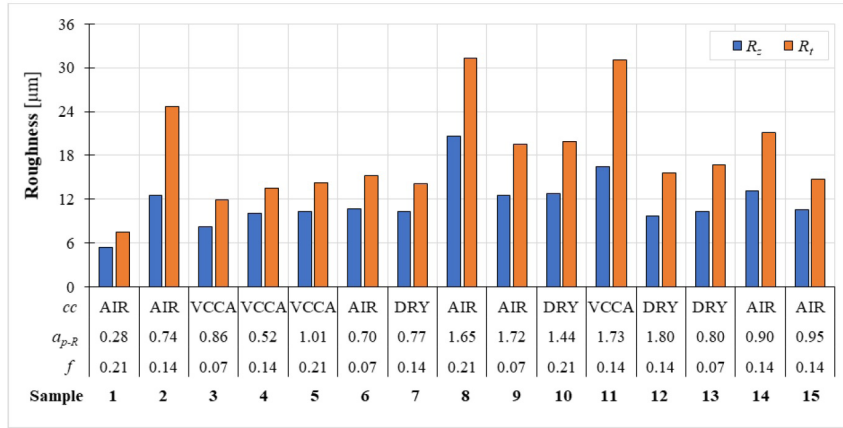
(b)

Figure 3. Roughness values for each combination of cutting parameters: (a) R_a and R_q; (b) R_z and R_t.

3. Results and Discussions

Figure 3 presents the arithmetic means of R_a, R_q, R_z, and R_t for the tested samples. Direct comparison between samples 1 and 8 ($f = 0.21$ mm/rev; AIR condition) shows a significant growth of roughness values as the real value of axial depth of cut ($a_{p\text{-}R}$) increases from 0.28 to 1.65 μm, indicating an influence of a_p in the surface roughness for high feed rates. Other authors presented similar results. Sreenivasulu[20] observed that the increase in a_p harmed the surface quality in GFRP milling. Zhou et al.[26] concluded that a_p is the most influential factor in roughness values, and its increase worsens the quality of the surface machined in CFRP. According to the authors, the several layers of epoxy resin are difficult to remove; in this case, most of these can adhere to the machined surface due to the combined effect of the force and heat generated

by the tool's action. El-Hofy et al.[29] also observed a leap in temperature when increasing the axial cutting depth: when growing a_p from 1.0 to 3.0 mm, the temperature rose from 70 to 170 °C. Direct comparison between samples 2 and 7 ($f = 0.14$ mm/rev and $a_{p\text{-}R} = 0.75$ mm), in which the cooling condition is changed from AIR to DRY, shows an increase in all roughness parameters for DRY machining. However, the surface roughness on samples 11 and 12 ($f = 0.14$ mm/rev and $a_{p\text{-}R} = 1.75$ mm) increases when changing from DRY to VCCA. Therefore, the application of compressed air (AIR and VCCA) increases the R_a, R_q, R_z, and R_t values as a_p rises because it generates more heat in the cutting zone that produces growth in the material temperature, higher tool wear, less support of the matrix resin for the fibers, and lower surface quality[18-20,25,26,46].

Table 2 presents the reduced ANOVA of R_a, R_q, R_z, and R_t values for a 95% confidence interval. The results show that the quadratic effect of axial depth of cut ($a_p{}^2$) and its combined effect with feed rate ($f \times a_p$) are the most significant factors for both R_a and R_z (contributions close to 30%). The combined effect a_p x cc also stands out, significantly influencing R_a and R_z (contributions of 19.2% and 11.7%, respectively). The linear effect of feed rate (f) and the quadratic effect of the cooling condition (cc^2) are also significant factors but with a minor contribution.

The model representing the responses (Y) can be described as functions of f, a_p and cc and is expressed by Equation 1. Equations 2 to 5 present the regression models for R_a, R_q, R_z, and R_t. Since the coefficients of determination (R^2) are greater than 70%, the regression model fits well the experimental data.

$$Y = b_0 + b_1(f) + b_2(a_p{}^2) + b_3(cc^2) + b_4(a_p \times f) + b_5(a_p \times cc) \quad (1)$$

$$R_a = 2.098 - 0.786(f) + 0.027(a_p{}^2) - 0.689(cc^2) + 0.293(a_p \times f) + 0.118(a_p \times cc) \quad (2)$$

$$R_q = 2.58 - 0.90(f) + 0.03(a_p{}^2) + 0.79(cc^2) + 0.34(a_p \times f) + 0.14(a_p \times cc) \quad (3)$$

$$R_z = 10.927 - 3.28(f) + 0.116(a_p{}^2) - 2.40(cc^2) + 1.225(a_p \times f) + 0.385(a_p \times cc) \quad (4)$$

$$R_t = 14.52 - 4.58(f) + 0.22(a_p{}^2) + 1.66(a_p \times f) + 0.84(a_p \times cc) \quad (5)$$

The results found in the ANOVA for all roughness parameters were similar, with the quadratic effect of axial depth of cut ($a_p{}^2$) and the interaction between the axial depth of cut and the feed rate (a_p x f) presenting the most significant influences (these factors showed the smallest P-values and thus the most important contributions). In addition, the interaction a_p x cc also contributed strongly to all the roughness parameters evaluated. The behavior of the average roughness R_a for the significant controllable factors is shown in Figure 4. The behaviors of the other roughness parameters evaluated (R_q, R_z and R_t) were similar to those observed for R_a.

Table 2. Reduced ANOVA ($\alpha = 0.05$).

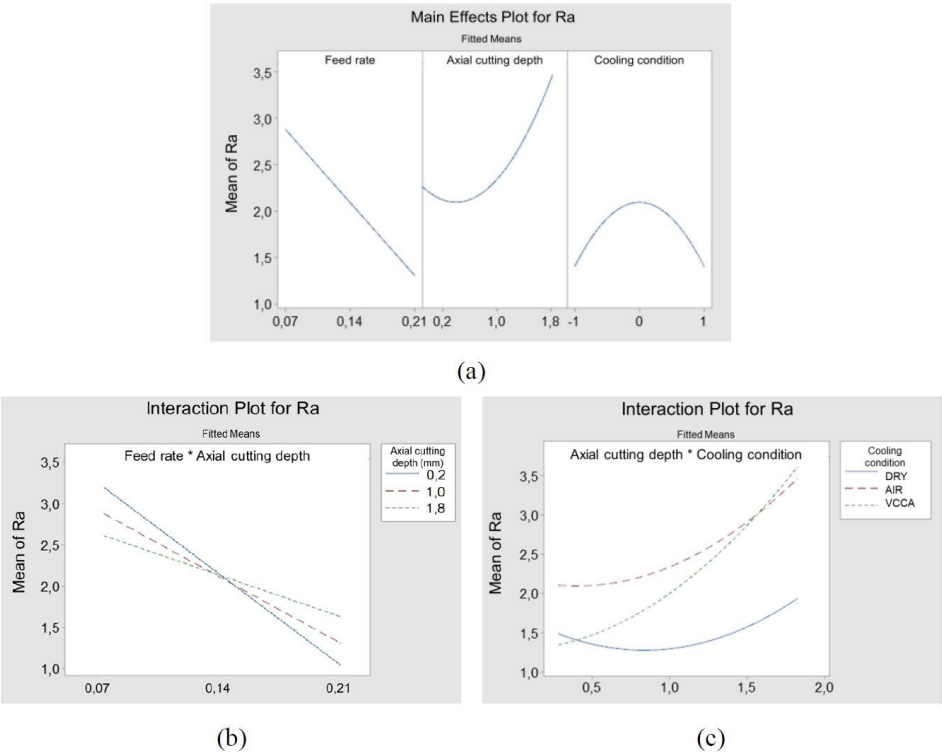| Factors	R_a		R_q		R_z		R_t	
	P-value	Contrib.	P-value	Contrib.	P-value	Contrib.	P-value	Contrib.
f	0.007	3.7%	0.014	4.3%	0.021	4.0%	0.072	1.9%
$a_p{}^2$	0.001	26.0%	0.001	27.5%	0.002	29.8%	0.006	31.5%
cc^2	0.007	8.8%	0.012	7.9%	0.041	4.9%	0.115	4.4%
a_p x f	0.001	30.1%	0.001	28.7%	0.002	31.2%	0.019	20.6%
a_p x cc	0.005	19.2%	0.009	17.5%	0.040	11.7%	0.056	14.6%
R^2	87.7%		85.8%		81.7%		72.8%	

(a)

(b)

(c)

Figure 4. Graphs of significant factors of R_a: (a) main effects; (b) effect of the a_p x f interaction; (c) effect of the a_p x cc interaction.

Figure 5 presents the 3D surface plots for R_a and R_t. R_q and R_z behaved similarly to R_a for the three control variables (f, a_p, cc). Values of a_{p-R} low (0.3 - 0.8 mm), medium (0.8 - 1.4 mm), and high (1.4 - 1.8 mm) were considered. The quadratic effect of a_p is evident since, at low values of a_p, the value of R_a decreases with the increase of f (runs 6 and 1) by about 45% (from 2.21 μm to 0.96 μm) and about 50% (from 15.24 μm to 7.53 μm) for R_t. The results of R_a for DRY and VCCA machining distinguish themselves from the results obtained with the AIR condition: the latter presents higher values of average roughness R_a. This behavior was not observed for the total height of the roughness profile R_t, wherein the three types of cc have similar values. The most probable cause for this inconsistent behavior lies in the definition of the roughness parameters. While the mean roughness R_a is an arithmetic mean of the absolute values of the profile, the total height of the roughness profile R_t

is the distance between the highest peak and the deepest valley in the evaluation length. Thus, while the influence of eventual defects caused by fiber pullout or delamination is softened in R_a, the occurrence of several defects may affect this parameter more significantly. On the other hand, the frequency of defects in the evaluation length tends to have a weaker influence on R_t since only the highest peak and the deepest valley are considered.

For the lowest a_{p-R}, increasing f resulted in smaller values for all roughness parameters (samples 6 and 1): R_a presented a decrease of about 55% (from 2.20 μm to 0.96 μm), and R_t reduction was around 50% (from 15.24 μm to 7.53 μm). For high a_{p-R}, the increase of feed rate (samples 9 and 8) almost doubled the resulting R_a (from 2.27 μm to 4.5 μm) and increased R_t by approximately 60% (from 19.48 μm to 31.30 μm). An equivalent result was found by Kiliçkap et al.[22]. Furthermore, distinct behaviors were observed for the
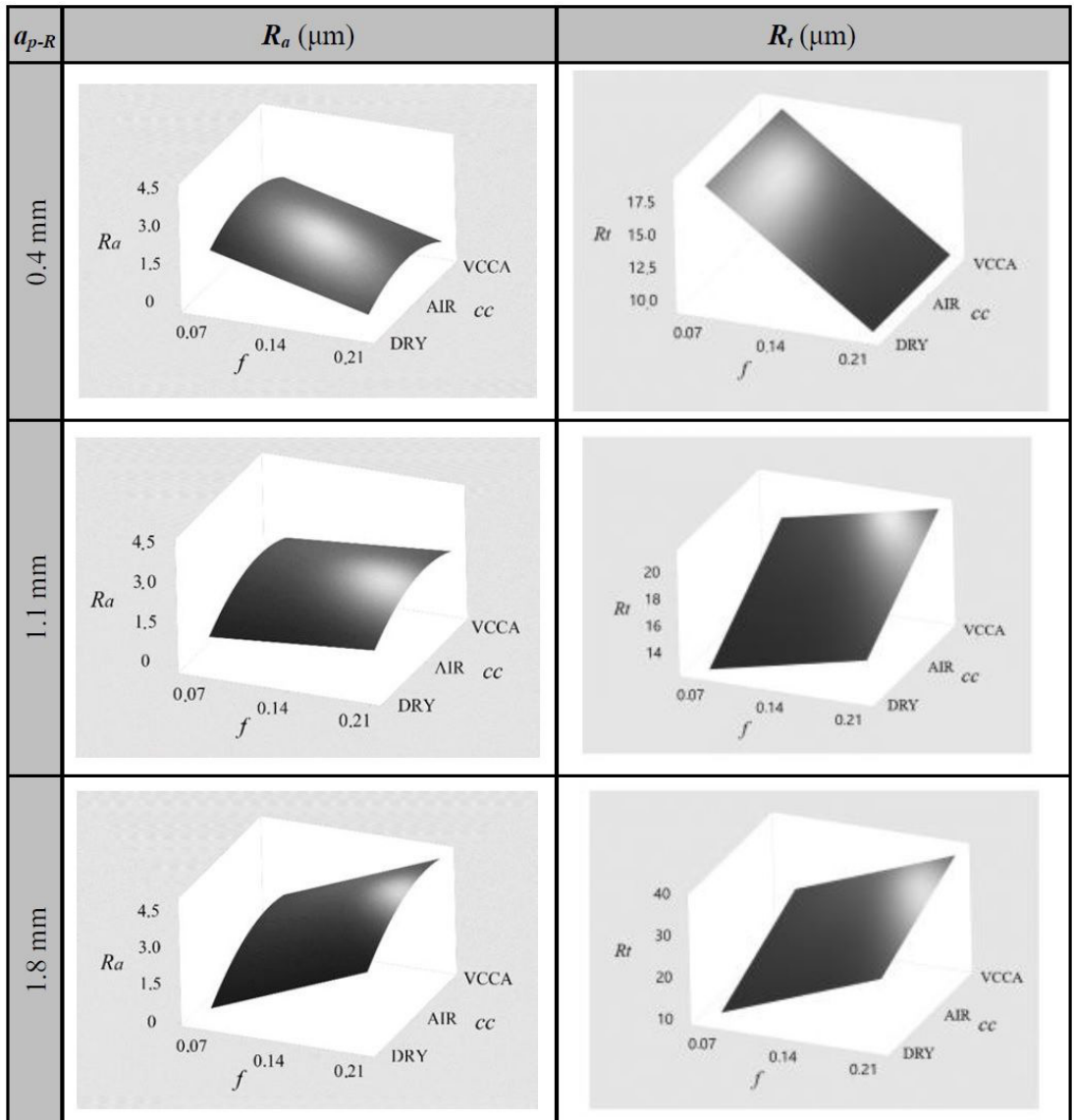

Figure 5. R_a and R_t surface graphics.

different cc, with AIR presenting the worst outcomes for R_a and VCCA the worst results for R_t.

The plot behaviors of Figure 5 indicate an inflection point on the regression model for a_p, with the feed rate affecting the surface roughness differently for each extremity, which reinforces the significant influence of a_p^2 demonstrated by the ANOVA. This inflection point varied from 0.90 mm to 0.95 mm for the different surface roughness parameters evaluated. Thus, $a_p = 0.90$ mm was considered the value of depth of cut in which the feed rate presented negligible influence (Figure 6). Below this point, the increase of f reduces the roughness values; above this a_p, the rise of f increases these values. Otherwise, when a low feed rate ($f = 0.07$ mm/rev) is used with AIR (samples 6 and 9), the growth of a_p affected only marginally the roughness values.

For high a_p values, DRY produced lower roughness values. The use of VCCA shows good results only for low a_p. The use of AIR generated worse results than VCCA with low a_p and worse outcomes than DRY with high a_p; however, the analysis of variance indicates that the differences observed are not statistically significant. As followed by Gao et al.[25], the damage caused is possibly related to the cutting forces: high a_p values result in higher forces that are yet increased with VCCA. For low a_p values, the force might not be large enough to allow the cut without pulling out of fibers, and the increase of the matrix stiffness caused by VCCA contributes to improving the surface roughness. Something that reinforces this theory is the behavior of the feed rate (f). On the other hand, due to the higher temperatures, the cut of the polymer matrix is easier with DRY milling than

for VCCA-assisted milling, where higher cutting forces are expected. However, the incidence of fiber pullout is less common in VCCA-assisted milling than in AIR and DRY cutting, which is evidenced by cavities and higher R_t values in AIR and DRY cutting. This effect was also observed by Morkavuk et al.[8].

According to Figure 5, with low a_p, the highest tested feed rate (0.21 mm/rev) is feasible; however, for high a_p values, low roughness values are observed for low feed rates (0.07 mm/rev) – in this case, increasing f heightens radial cutting forces[57]. Jia et al.[58] also mention that low temperatures raise the cutting forces. The resin matrix softens under high temperatures, thus weakening the fiber support and reducing the cohesive strength of the fiber matrix. Therefore, being mainly pressed by the cutting edge, the fiber and resin matrix peel off easily, and severe folds of the fiber occur under the cutting plane. Comparatively, as the resin matrix hardens under low temperatures, the support of the resin matrix becomes strong, which contributes to the slight deformation of the fibers before cutting. Therefore, the fibers and the resin matrix are compressed by the exit surface of the cutting tool, inducing small folds in the fibers and cracks in the resin matrix. Moreover, the fibers are fractured close to the cutting plane with small shear angles.

Figure 7 presents SEM images of the machined surfaces of sample 1 ($f = 0.21$ mm/rev, $a_{p-R} = 0.28$ mm, and AIR). SEM images show a homogeneous and opaquer surface, with low roughness values, composed mainly of non-fractured carbon fibers. Only microscale damages were identified. On the other hand, Figure 8 presents an irregular surface
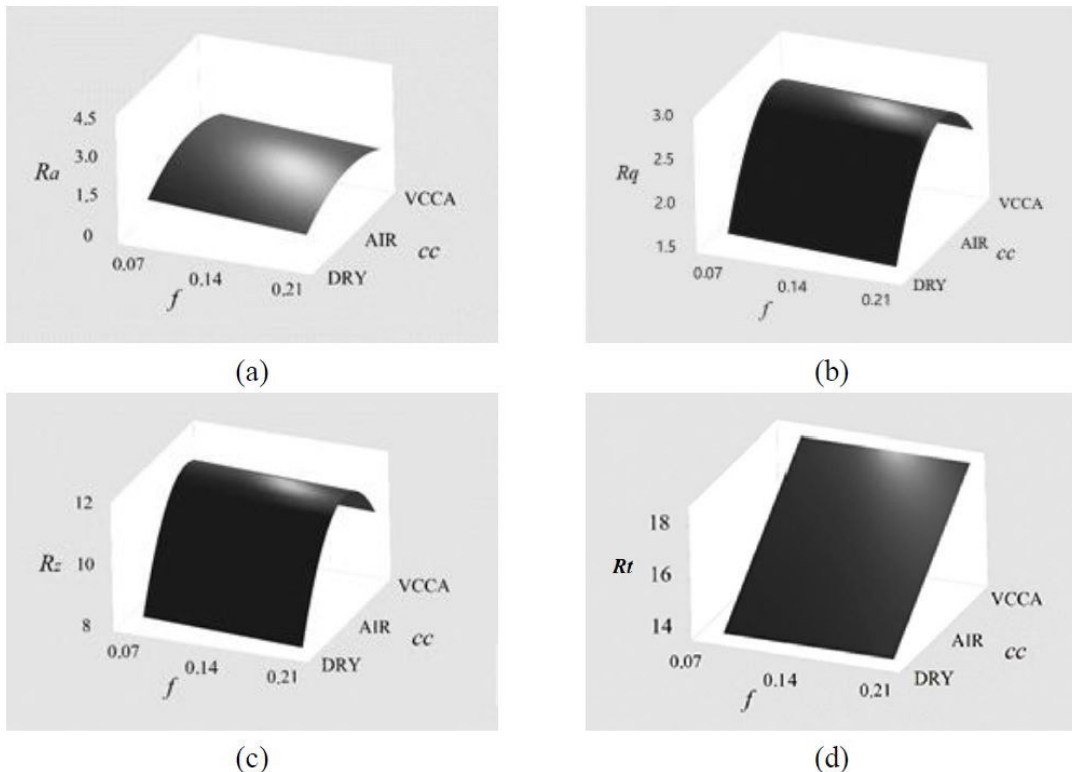
(a)

(b)

(c)

(d)

Figure 6. Surface plots in the inflection point ($a_p = 0{,}9$ mm): (a) R_a; (b) R_q; (c) R_z; (d) R_t.
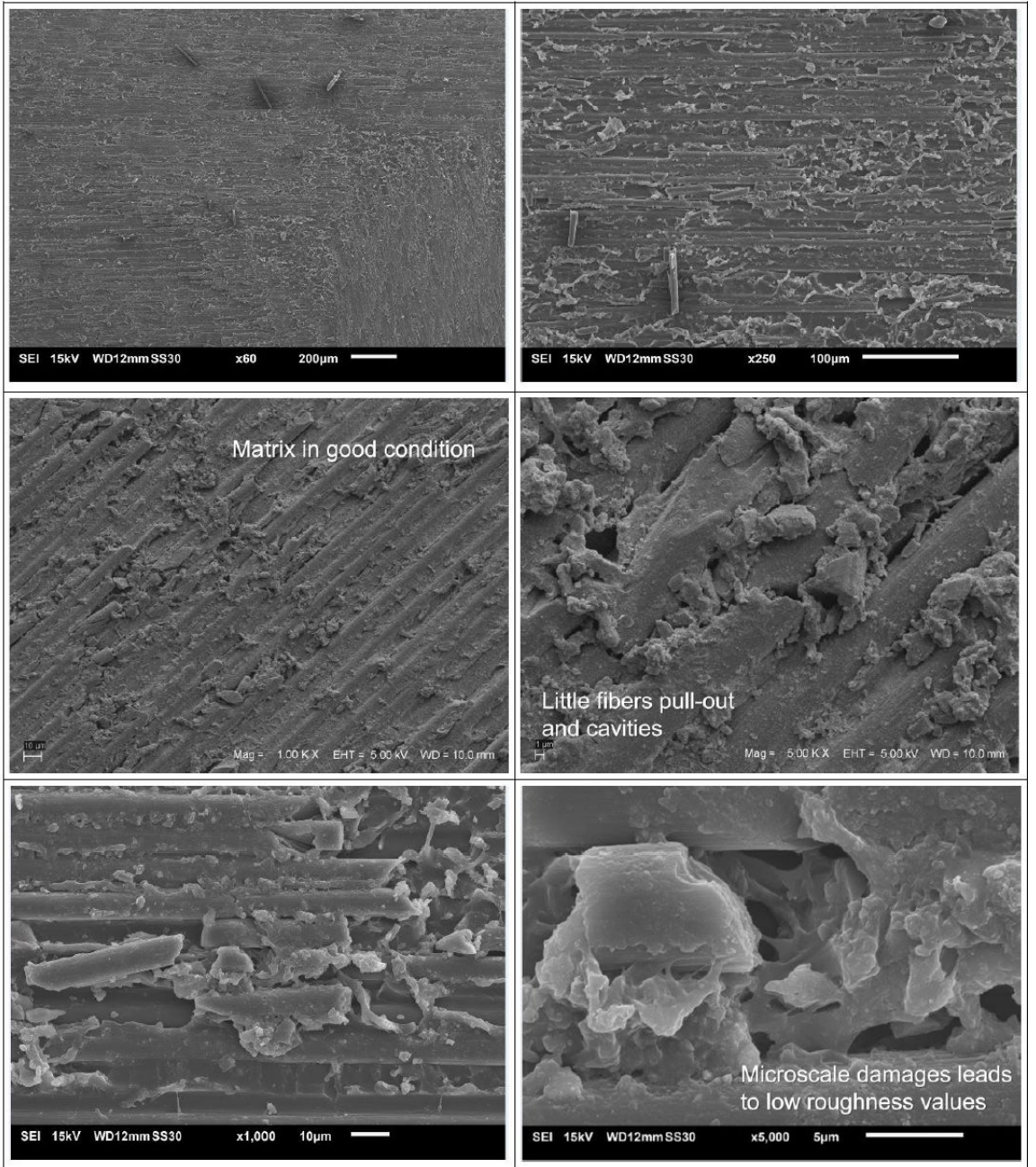
Figure 7. SEM images of sample 1.

with high roughness values, fractured fibers, adhered matrix material, and exposed resin resulting from the machining of sample 8, in which a_{p-R} was increased to 1.65 mm (other conditions, including cooling, were identical to sample 1). Gao et al.[25] explain that this failure occurs because the fiber and matrix separate due to the interphasic disconnection caused by the tool when it enters the workpiece at the 0º angle. The separation is propagated with the feed rate that causes bending and compression stress in the fiber and matrix until the fiber reaches a critical length, and its rupture happens at an angle close to 90º, exposing the matrix.

The roughness profile of sample 1 is presented in Figure 9a. This profile has relatively low peaks and valleys, resulting in low roughness values ($R_a = 0.96$ μm, $R_q = 1.21$ μm, $R_z = 5.39$ μm, and $R_t = 7.53$ μm) precisely because the generated surface has homogeneous and non-fractured carbon fibers, without apparent fiber pullouts. On the other hand, the roughness profile of sample 8 (Figure 9b) is very irregular, with high peaks and valleys, a condition observed by Gao et al.[25]. This condition resulted in high roughness values ($R_a = 4.5$ μm, $R_q = 5.46$ μm, $R_z = 20.6$ μm, and $R_t = 31.3$ μm) described by the fracture of carbon fibers and the resin exposure for
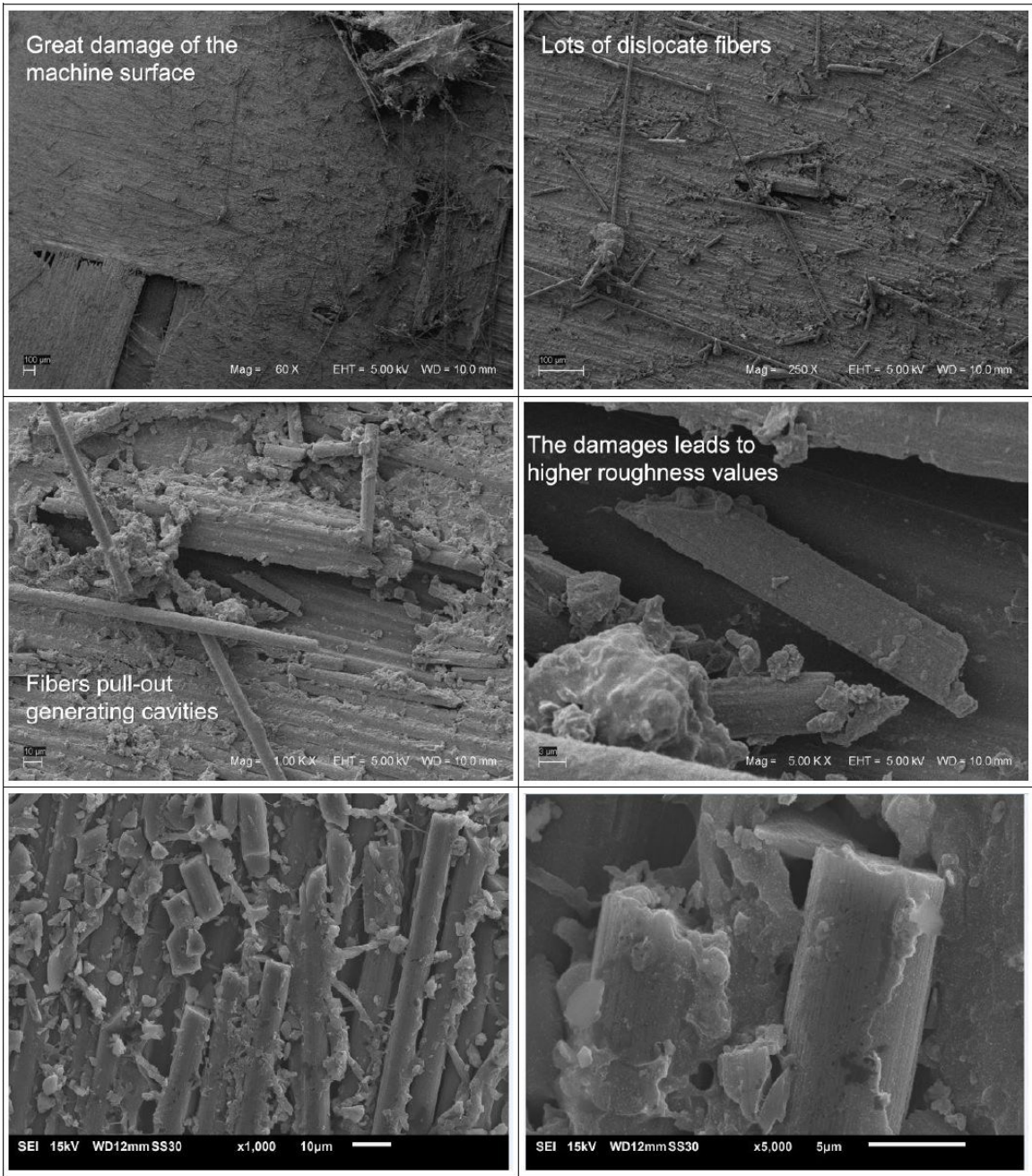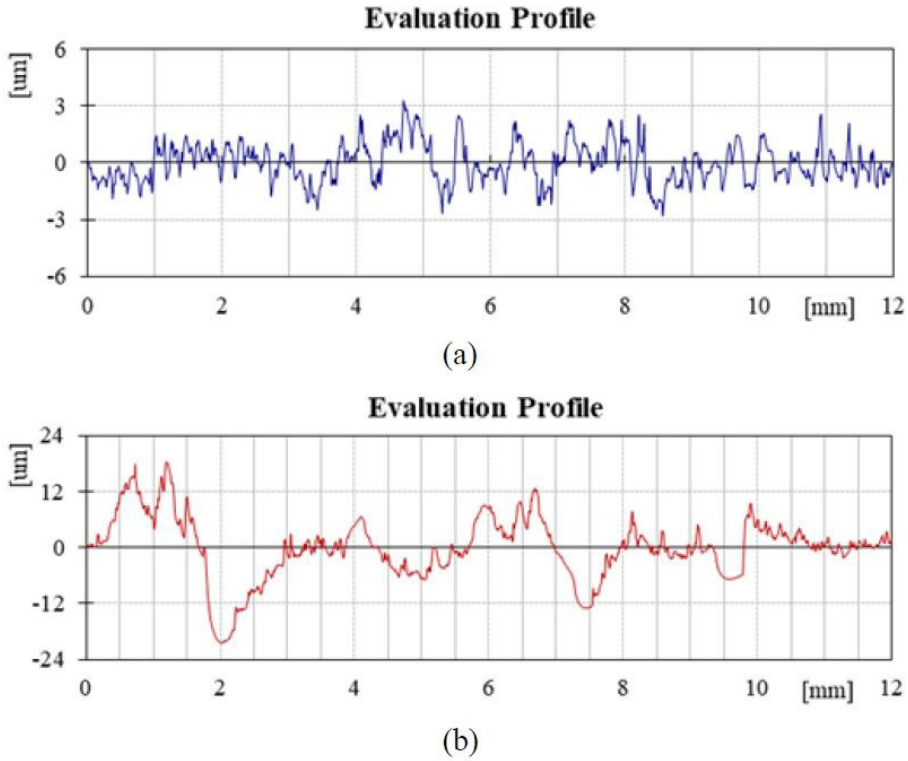
Figure 8. SEM images of sample 8.

machining tests using a_{p-R} = 1.65 mm. Nor Khairusshima and Sharifah[45] observed higher thermal stresses associated with the increase of a_p, resulting in worse surface quality.

The control variables were optimized from the multivariate analysis, and the ideal condition was a_{p-T} = 0.6 mm, f = 0.21 mm/rev, and VCCA. Since DRY and VCCA generated roughness values lower than AIR, it was decided to seek optimized conditions for both DRY and VCCA; thus, two sets of validation experiments (three runs each) were carried out, one for each cooling situation. It is worth be noted that the optimization resulted in different values of a_{p-R} for the DRY and VCCA

(Table 3). The optimization of the input parameters resulted in low mean roughness values: even with a significantly higher a_{p-T}, optimized results with VCCA only second those obtained in the machining of sample 1 (a_{p-R} = 0.28 mm). Run 3 (a_{p-R} = 0.86 mm, f = 0.07 mm/rev and VCCA) presented R_a, R_q, R_z, and R_t values close to those obtained with the optimized parameters (1.68 μm, 2.02 μm, 8.18 μm, and 11.86 μm respectively). The roughness values obtained using the optimized conditions for DRY machining were significantly higher than those obtained with VCCA milling, even with the higher a_{p-T} used with VCCA milling. Similar

Table 3. Validation test.

Runs	a_{p-R} (mm)	cc	R_a (µm)	R_q (µm)	R_z (µm)	R_t (µm)
16	0.50		2.34	2.93	13.43	27.25
17	0.60	DRY	2.20	2.73	12.75	17.98
18	0.65		1.95	2.43	11.75	19.78
Mean	0.60		2.16	2.70	12.64	21.67
19	0.76		1.65	2.03	9.42	13.95
20	0.80	VCCA	1.45	1.84	8.86	12.78
21	0.84		1.64	2.07	9.90	14.17
Mean	0.80		1.58	1.98	9.39	13.63

Figure 9. Machined roughness profiles: (a) sample 1; (b) sample 8.

behavior was also observed by Nor Khairusshima et al.[19]. As aforementioned, the feed rate did not significantly influence the results for a_p = 0.8 mm.

Figure 10 presents SEM images of the CFRP machined surface with the optimum conditions for VCCA-assisted milling. Despite using a significantly higher a_{p-R} (0.8 mm), the surface is homogeneous and very similar to the observed for sample 1 (a_{p-R} = 0.28 mm). The roughness profile of sample 20 is presented in Figure 11. Small peaks and valleys (close to 2 µm) are identified, matching the low roughness values measured.

Previous studies involving the machining of CFRP and other fiber-reinforced composites were developed by the author's research group. Initial studies approached the drilling of metal-composite stack[31] and CFRP[44]. While Devitte et al.[31] studied the optimization of the drilling process, Hoffmann et al.[44] evaluated the influence of VCCA on the quality of drilled holes. A study of the temperature

in the drilling process was performed by Devitte et al.[39], which reported temperatures well below the degradation temperature for the tested conditions, with an analysis of SEM images indicating the absence of fiber deformation and matrix degradation. The influence of the cutting parameters and VCCA on the surface finish of CFRP parts after end milling with carbide tools was formerly studied by Klein et al.[47]. A strong influence was observed for the depth of cut and its combined effect with feed rate and the cooling condition on the surface roughness. However, the paper focused on R_a and R_z parameters, disregarding the total roughness (R_t). In the current paper, a deeper investigation is carried out, including the behavior of R_t and further SEM analysis. Since R_t is more sensitive to damages in the machined surface than other roughness parameters (as depicted for runs 2 and 11 in Figure 3), it is a valuable parameter for evaluating the CFRP machined surface quality.
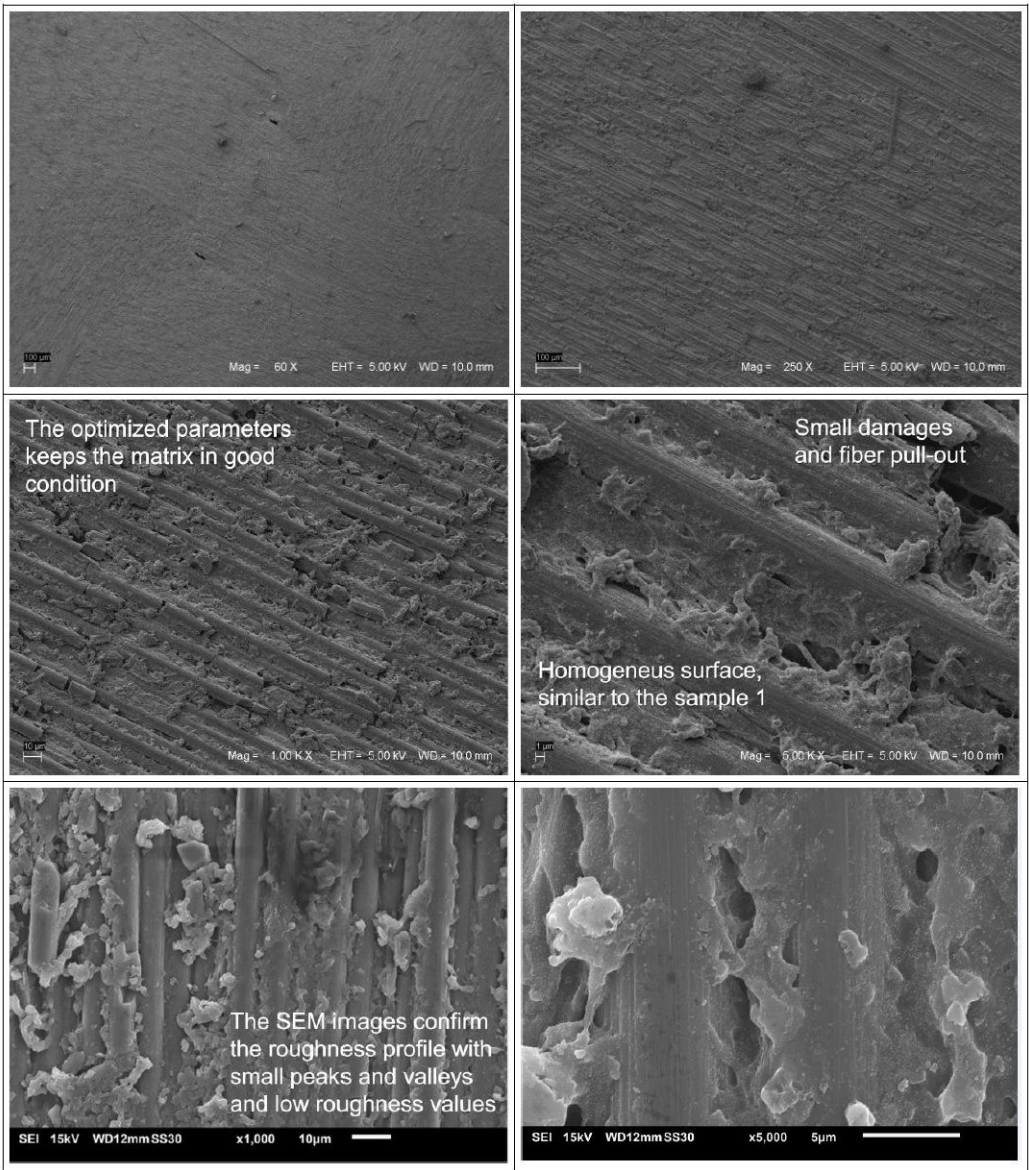
Figure 10. SEM images of the machined surface of sample 20.

Figure 11. Roughness profile of the machined surface of sample 20.

4. Conclusions

After analyzing the experimental results for the end milling of CFRP with a 4-flute end mill tool with different levels of axial depth of cut (a_p), feed rate (f), and cooling condition (cc) using the Box-Behnken Design, the following conclusions regarding the machined surface quality were drawn:

- The quadratic effect of a_p and the interactions of a_p with f and cc were the most significant factors influencing surface roughness. The combined influence of these factors presented a contribution of around 70% for the evaluated surface roughness parameters (R_a, R_q, R_z and R_t values).
- There is an inflection point at $a_p = 0.9$ mm, in which f does not influence the roughness values. When $a_p < 0.9$ mm, these values decrease with increasing f; but, for $a_p > 0.9$ mm, the values grow with increasing f, demonstrating the quadratic effect of a_p.
- The increase of a_p results in higher roughness values for AIR and VCCA-assisted milling. Tests performed with DRY cutting demonstrated a lower influence of a_p in the surface roughness: the heat generation during machining softens the matrix, favoring the cut and generating smaller R_a and R_q values than VCCA. However, reduced stiffness of the matrix material at high temperatures tends to cause fiber pullouts that do not occur with VCCA, resulting in higher R_z and R_t values.
- Optimized machining parameters resulted in lower roughness values for VCCA-assisted milling than DRY milling.
- The depth of cut presented a strong influence on the machined surface roughness of the CFRP, with higher depths of cut leading to worse surface finishes. This influence is evidenced by the occurrence of defects like fiber pullout, cavities, and adherence of material from the matrix.

5. Acknowledgments

6. References

1. Campbell FC Jr, editor. Manufacturing processes for advanced composites. Burlington: Elsevier; 2003.
2. Callister WD Jr, Rethwisch DG. Fundamentals of materials science and engineering: an integrated approach. Hoboken: John Wiley & Sons; 2012.
3. Ozkan D, Gok MS, Oge M, Karaoglanli AC. Milling behavior analysis of carbon fiber-reinforced polymer (CFRP) composites. Mater Today: Proc. 2019;11:526-33.
4. Chen Y, Guo X, Zhang K, Guo D, Zhou C, Gai L. Study on surface quality of CFRP machined by micro-textured milling tools. J Manuf Process. 2019;37:114-23.
5. Davim JP, editor. Machining: fundamentals and recent advances. London: Springer Science & Business Media; 2008.
6. Mallick PK. Fiber-reinforced composites: materials, manufacturing, and design. New York: CRC Press; 2007.
7. Koplev A, Lystrup A, Vorm T. The cutting process, chips, and cutting forces in machining CFRP. Composites. 1983;14(4):371-6.
8. Morkavuk S, Köklü U, Bağcı M, Gemi L. Cryogenic machining of carbon fiber reinforced plastic (CFRP) composites and the effects of cryogenic treatment on tensile properties: a comparative study. Compos, Part B Eng. 2018;147:1-11.
9. Hintze W, Hartmann D, Schutte C. Occurrence and propagation of delamination during the machining of carbon fibre reinforced plastics (CFRPs): an experimental study. Compos Sci Technol. 2011;71(15):1719-26.
10. Martins FR. Characterization of milling carbon fiber reinforced polymer composite sheets (CFRP) [thesis]. Campinas: Universidade Estadual de Campinas; 2014 (in Portuguese).
11. Ferreira JR, Coppini NL, Miranda GWA. Machining optimisation in carbon fibre reinforced composite materials. J Mater Process Technol. 1999;92-93:135-40.
12. Teti R. Machining of composite materials. CIRP Ann. 2002;51(2):611-34.
13. Grilo TJ, Paulo RMF, Silva CRM, Davim JP. Experimental delamination analyses of CFRPs using different drill geometries. Compos, Part B Eng. 2013;45(1):1344-50.
14. Dandekar CR, Shin YC. Modeling of machining of composite materials: a review. Int J Mach Tools Manuf. 2012;57:102-21.
15. Haeger A, Schoen G, Lissek F, Meinhard D, Kaufeld M, Schneider G, et al. Non-destructive detection of drilling-induced delamination in CFRP and its effect on mechanical properties. Procedia Eng. 2016;149:130-42.
16. Karataş MA, Gökkaya H. A review on machinability of carbon fiber reinforced polymer (CFRP) and glass fiber reinforced polymer (GFRP) composite materials. Defence Technol. 2018;14(4):318-26.
17. He Y, Qing H, Zhang S, Wang D, Zhu S. The cutting force and defect analysis in milling of carbon fiber-reinforced polymer (CFRP) composite. Int J Adv Manuf Technol. 2017;93(5-8):1829-42.
18. Voss R, Seeholzer L, Kuster F, Wegener K. Influence of fibre orientation, tool geometry and process parameters on surface quality in milling of CFRP. J Manuf Sci Technol. 2017;18:75-91.
19. Nor Khairusshima MK, Che Hassan CH, Jaharah AG, Amin AKM, Md Idriss AN. Effect of chilled air on tool wear and workpiece quality during milling of carbon fibre-reinforced plastic. Wear. 2013;302(1-2):1113-23.
20. Sreenivasulu R. Optimization of surface roughness and delamination damage of GFRP composite material in end milling using Taguchi design method and artificial neural network. Procedia Eng. 2013;64:785-94.
21. Azmi AI, Lin RJT, Bhattacharyya D. Machinability study of glass fibre-reinforced polymer composites during end milling. Int J Adv Manuf Technol. 2013;64(1-4):247-61.
22. Kiliçkap E, Yardimeden A, Çelik YH. Investigation of experimental study of end milling of CFRP composite. Sci Eng Compos Mater. 2015;22(1):89-95.
23. Wang C, Liu G, An Q, Chen M. Occurrence and formation mechanism of surface cavity defects during orthogonal milling of CFRP laminates. Compos, Part B Eng. 2017;109:10-22.
24. Pecat O, Rentsch R, Brinksmeier E. Influence of milling process parameters on the surface integrity of CFRP. Procedia CIRP. 2012;1:466-70.
25. Gao C, Xiao J, Xu J, Ke Y. Factor analysis of machining parameters of fiber-reinforced polymer composites based on finite element simulation with experimental investigation. Int J Adv Manuf Technol. 2016;83(5-8):1113-25.
26. Zhou JW, Chen Y, Fu YC, Xu JH, Hu AD, Liu SQ. Optimization of milling parameters of CFRP for surface roughness using Taguchi design method. Adv Mat Res. 2014;1027:76-9.

27. Çolak O, Sunar T. Cutting forces and 3D surface analysis of CFRP milling with PCD cutting tools. Procedia CIRP. 2016;45:75-8.

28. Yashiro T, Ogawa T, Sasahara H. Temperature measurement of cutting tool and machined surface layer in milling of CFRP. Int J Mach Tools Manuf. 2013;70:63-9.

29. El-Hofy MH, Soo SL, Aspinwall DK, Sim WM, Pearson D, M'Saoubi R, et al. Tool temperature in slotting of CFRP composites. Procedia Manuf. 2017;10:371-81.

30. Nor Khairusshima MN, Ch CH, Jaharah AG, Akm NA. Tool wear and surface roughness on milling carbon fiber-reinforced plastic using chilled air. J Asian Sci Res. 2012;2:593.

31. Devitte C, Souza GSC, Souza AJ, Tita V. Optimization for drilling process of metal-composite aeronautical structures. Sci Eng Compos Mater. 2021;28(1):264-75.

32. Wang H, Sun J, Zhang D, Guo K, Li J. The effect of cutting temperature in milling of carbon fiber reinforced polymer composites. Compos, Part A Appl Sci Manuf. 2016;91:380-7.

33. Kim M, Lee M, Cho G, Lee S. Effect of the fiber orientation and the radial depth of cut on the flank wear in end milling of CFRP. Int J Precis Eng Manuf. 2020;21(7):1187-99.

34. Wang X, Kwon PY, Sturtevant C, Kim DD-W, Lantrip J. Tool wear of coated drills in drilling CFRP. J Manuf Process. 2013;15(1):127-35.

35. Akay M. Aspects of dynamic mechanical analysis in polymeric composites. Compos Sci Technol. 1993;47(4):419-23.

36. Ben W, Hang G, Quan W, Maoqing W, Songpeng Z. Influence of cutting heat on quality of drilling of carbon/epoxy composites. Mater Manuf Process. 2012;27(9):968-72.

37. Fu R, Jia Z, Wang F, Jin Y, Sun D, Yang L, et al. Drill-exit temperature characteristics in drilling of UD and MD CFRP composites based on infrared thermography. Int J Mach Tools Manuf. 2018;135:24-37.

38. Ha SJ, Kim KB, Yang JK, Cho MW. Influence of cutting temperature on carbon fiber-reinforced plastic composites in high-speed machining. J Mech Sci Technol. 2017;31(4):1861-7.

39. Devitte C, Souza AJ, Schirmer GV. Temperature evaluation in CFRP drilling. In: 5th Brazilian Conference on Composite Materials (BCCM 5); 2021 Jan 18-22; São Carlos, SP, Brazil. Proceedings. São Carlos: EESC-USP; 2021.

40. Kim C, Cho CH, Son I, Lee H, Han JW, Kim JG, et al. Effect of microscale oil penetration on mechanical and chemical properties of carbon fiber-reinforced epoxy composites. J Ind Eng Chem. 2018;61:112-8.

41. Rodriguez RL, Lopes JC, Mancini SD, Ângelo Sanchez LE, Varasquim FMFA, Volpato RS, et al. Contribution for minimization the usage of cutting fluids in CFRP grinding. Int J Adv Manuf Technol. 2019;103(1-4):487-97.

42. Xu J, Ji M, Davim JP, Chen M, El Mansori M, Krishnaraj V. Comparative study of minimum quantity lubrication and dry drilling of CFRP/titanium stacks using TiAlN and diamond coated drills. Compos Struct. 2020;234:111727.

43. Dixit US, Sarma DK, Davim JP. Environmentally friendly machining. Boston: Springer Science & Business Media; 2012.

44. Hoffmann N, Souza GSC, Souza AJ, Tita V. Delamination and hole wall roughness evaluation in air-cooled drilling of carbon fiber-reinforced polymer. J Compos Mater. 2021;55(23):3161-74.

45. Nor Khairusshima MK, Sharifah ISS. Study on tool wear during milling CFRP under dry and chilled air machining. Procedia Eng. 2017;184:506-17.

46. Yalçın B, Özgür AE, Koru M. The effects of various cooling strategies on surface roughness and tool wear during soft materials milling. Mater Des. 2009;30(3):896-9.

47. Klein RF, Hoffmann N, Pereira WAF, Souza AJ. Effects of vortex-cooled compressed air on surface quality in end-milling CFRP. In: 5th Brazilian Conference on Composite Materials (BCCM 5); 2021 Jan 18-22; São Carlos, SP, Brazil. Proceedings. São Carlos: EESC-USP; 2021.

48. Sheikh-Ahmad JY. Machining of polymer composites. New York: Springer; 2009.

49. Klocke F, Kuchle A. Manufacturing processes. Berlin: Springer; 2009.

50. Nguyen-Dinh N, Hejjaji A, Zitoune R, Bouvet C, Salem M. New tool for reduction of harmful particulate dispersion and to improve machining quality when trimming carbon/epoxy composites. Compos, Part A Appl Sci Manuf. 2020;131:105806.

51. Gara S, Tsoumarev O. Prediction of surface roughness in slotting of CFRP. Measurement. 2016;91:414-20.

52. Chatelain JF, Zaghbani I, Monier J. Effect of ply orientation on roughness for the trimming process of CFRP laminates. Int J Ind Manuf Eng. 2012;6:1516-22.

53. Policena MR, Devitte C, Fronza G, Garcia RF, Souza AJ. Surface roughness analysis in finishing end-milling of duplex stainless steel UNS S32205. Int J Adv Manuf Technol. 2018;98(5-8):1617-25.

54. Konneh M, Izman S, Kassim AAR. Milling damage on carbon fibre reinforced polymer using TiAlN coated end mills. J Phys Conf Ser. 2015;628:012033.

55. Sankar BR, Umamaheswarrao P. Investigations on the surface roughness of drilled hole on carbon fiber reinforced plastic composite. In: Verma A, editor. Trends in industrial and mechanical engineering. New Delhi: Excellent Publishing House; 2016. p. 113-9.

56. Vinayagamoorthy R. Parametric optimization studies on drilling of sandwich composites using the Box-Behnken design. Mater Manuf Process. 2017;32(6):645-53.

57. Haiyan W, Xuda Q, Hao L, Chengzu R. Analysis of cutting forces in helical milling of carbon fiber-reinforced plastics. Proc Inst Mech Eng, B J Eng Manuf. 2013;227(1):62-74.

58. Jia Z, Fu R, Wang F, Qian B, He C. Temperature effects in end milling carbon fiber reinforced polymer composites. Polym Compos. 2018;39(2):437-47.